Streamline Curvature and Lift Generation

1 Momentum Equation on a Streamline

References:

1. http://web.mit.edu/16.unified/www/FALL/fluids/Fluids_Lectures/f20.pdf
2. Greitzer, Tan and Graf, *Internal Flow: Concepts and Applications*. Section 2.4

1.1 The ∇-operator

Recall the momentum equation in differential, vector form,

$$\rho \frac{D\vec{v}}{Dt} = -\nabla p + \rho \vec{F}_{\text{body}} + \vec{F}_{\text{visc}}$$

Assuming that,

- The flow is inviscid,
- The flow is steady,
- There are no body forces,

we arrive at,

$$\rho \left(\vec{v} \cdot \nabla\right) \vec{v} = -\nabla p \quad . \tag{1}$$

Remember that the ∇-operator is a vector operator. In Cartesian coordinates the operator is,

$$\nabla = \left(\mathbf{e}_x \frac{\partial}{\partial x} + \mathbf{e}_y \frac{\partial}{\partial y} + \mathbf{e}_z \frac{\partial}{\partial z} \right),$$

which is how we condense the x, y, and z momentum equations into one vector equation. In cylindrical coordinates, we would write the ∇-operator as,

$$\nabla = \left(\mathbf{e}_r \frac{\partial}{\partial r} + \mathbf{e}_\theta \frac{1}{r} \frac{\partial}{\partial \theta} + \mathbf{e}_z \frac{\partial}{\partial z} \right).$$

We could also write out the ∇-operator for spherical coordinates or any other coordinate system. Let us consider an orthogonal coordinate system that is aligned with the streamlines of the flow.

1.2 Natural Coordinates

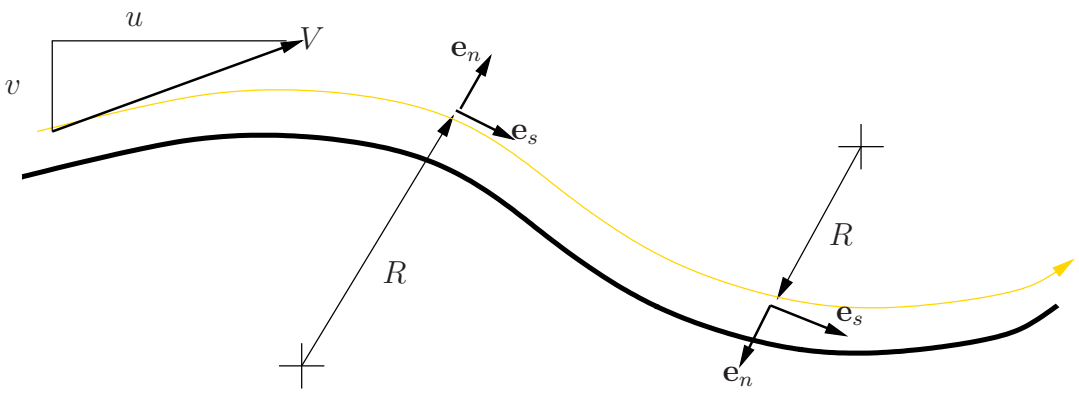

Figure 1: The streamline (natural) coordinate system, $(\mathbf{e}_s, \mathbf{e}_n, \mathbf{e}_b)$, where $\mathbf{e}_s$ is in the streamwise direction (tangent to the velocity vector) and $\mathbf{e}_n$ is normal to the streamwise direction along the radius of curvature

The streamline coordinate system, also called the *natural* coordinate system, is shown in Figure 1. The streamlines, and the streamwise unit vector, $\mathbf{e}_s$, are always tangent to the velocity vector. In the normal direction (also the radial direction), we have the unit vector, $\mathbf{e}_n$, and in the third orthogonal direction lies $\mathbf{e}_b$. The ∇-operator in this coordinate system is thus,

$$\nabla = \left(\mathbf{e}_s \frac{\partial}{\partial s} + \mathbf{e}_n \frac{\partial}{\partial n} + \mathbf{e}_b \frac{\partial}{\partial b} \right).$$

What does the momentum equation look like in this streamline coordinate system? To find out, we must first transform the velocity vector, $\vec{v}$, to streamline coordinates. In Cartesian coordinates,

the velocity vector is,

$$\vec{v} = (u\mathbf{e}_x + v\mathbf{e}_y + w\mathbf{e}_z)\,.$$

In streamline coordinates, the unit vector, $\mathbf{e}_s$, is by definition in the direction of the velocity vector. Thus,

$$\vec{v} = V\mathbf{e}_s, \qquad V = |\vec{v}| = \sqrt{u^2 + v^2 + w^2}.$$

Using this expression for the velocity vector in Equation 1,

$$\rho\,(V\mathbf{e}_s \cdot \nabla)\,V\mathbf{e}_s = -\nabla p \quad .$$

Let us expand the inertial term,

$$\begin{aligned}\rho\,(V\mathbf{e}_s \cdot \nabla)\,V\mathbf{e}_s &= \rho\left(V\frac{\partial}{\partial s}\right)V\mathbf{e}_s \\ &= \rho V\left(\frac{\partial V}{\partial s}\mathbf{e}_s + V\frac{\partial \mathbf{e}_s}{\partial s}\right)\end{aligned}$$

Here we have a derivative of a unit vector, which might seem odd at first glance. In Cartesian coordinates, the unit vectors and differential operators ($\frac{\partial}{\partial x}$, $\frac{\partial}{\partial y}$ and $\frac{\partial}{\partial z}$) are always aligned, so these derivatives are ignored. This is not necessarily true in other coordinate systems.

Let us investigate the change in the $\mathbf{e}_s$-direction over a small, streamwise step, ds, shown in Figure 2. The unit vector, $\mathbf{e}_s$, changes direction by $d\mathbf{e}_s$. This change is in the negative normal ($-\mathbf{e}_n$) direction and is of size, ϕ, assuming small angles. To relate ϕ to ds, consider the diagram in the lower right of Figure 2. The angle at point, C, must be $90° - d\theta$. Similarly, the angle at point, D, of triangle CBD is therefore $d\theta$, in the limit of small ds. This is the angle of change of the $\mathbf{e}_s$ unit vector ($\phi = d\theta$). Additionally, this angle can be related to ds by,

$$Rd\theta = ds$$

We can now write that,

$$\frac{\partial \mathbf{e}_s}{\partial s} = -\frac{1}{R}\mathbf{e}_n$$

Plugging this into the expression for the inertial term,

$$\rho\,(V\mathbf{e}_s \cdot \nabla)\,V\mathbf{e}_s = \rho\left[V\frac{\partial V}{\partial s}\mathbf{e}_s - \frac{V^2}{R}\mathbf{e}_n\right].$$

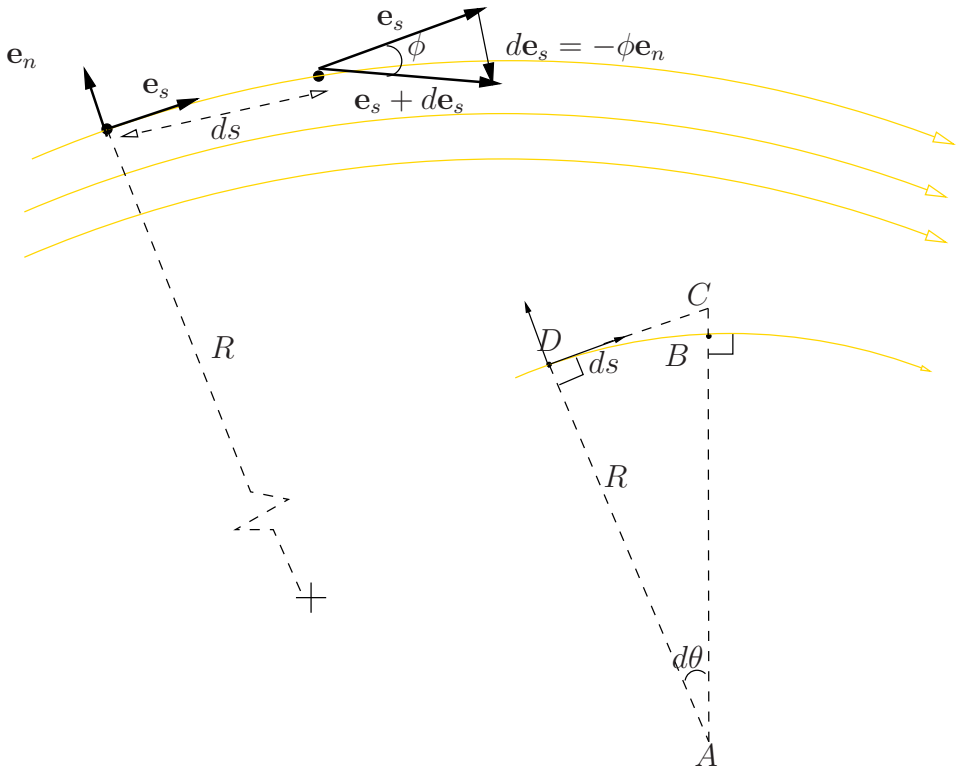

Figure 2: Change in $\mathbf{e}_s$ for a small streamwise step, ds.

Returning to the momentum equation in streamline coordinates, we have,

$$\rho\left[V\frac{\partial V}{\partial s}\mathbf{e}_s - \frac{V^2}{R}\mathbf{e}_n\right] = -\frac{\partial p}{\partial s}\mathbf{e}_s - \frac{\partial p}{\partial n}\mathbf{e}_n - \frac{\partial p}{\partial b}\mathbf{e}_b \quad .$$

Up to now we have only assumed steady, inviscid flow. If we also assume incompressible flow, then the above expression can be easily decomposed into the orthogonal directions,

$$\begin{aligned}
\frac{\partial}{\partial s}\left(p + \frac{1}{2}\rho V^2\right) &= 0 \\
\frac{\partial}{\partial n}\left(p \qquad\quad\right) &= \frac{\rho V^2}{R} \\
\frac{\partial}{\partial n}\left(p \qquad\quad\right) &= 0
\end{aligned}$$

Along a streamline we therefore have,

$$p + \frac{1}{2}\rho V^2 = Const.$$

This is the Bernoulli Equation! By transforming the momentum equation from Cartesian to streamline coordinates, we have recovered the Bernoulli equation.

Normal to the streamlines, we have that,

$$\frac{\partial p}{\partial n} = \frac{\rho V^2}{R} \quad ,$$

which states that the pressure gradient is related to the radius of curvature of the streamline. This is a statement valid for inviscid flows at any Mach number. This is a critical result that we will explore in more depth.

1.3 Streamline curvature and surface pressure

The above relation between pressure gradients and streamline curvature implies that changes in surface contours lead to changes in surface pressure. Consider the flow over a bump shown in Figure 3,

For a common ambient pressure, a concave curvature produces higher pressure near the wall and a convex curvature produces a lower wall pressure. Remember that the pressure gradient points in

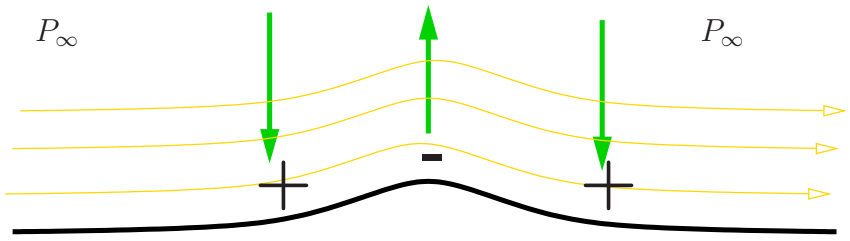

Figure 3: Surface pressure gradients for flow along a small bump.

the same direction as the radius of curvature. You can also think of the higher pressure pushing on the streamlines and forcing them to curve away.

The surface pressure variations over the bump are similar to those around an airfoil. Assuming a common, farfield, atmospheric pressure, the curvature of the streamlines allow us to derive the c_p and lift distributions around an airfoil.

2 Airfoil Pressure Distributions

This section seeks to understand the performance, specifically the lift performance and pressure distribution, of airfoils using streamline curvature. We take the perspective of an airfoil designer and closely examine the role of thickness and camber.

2.1 The Effect of Airfoil Thickness

The impact of thickness on the pressure distribution of an airfoil can be qualitatively observed by comparing two symmetric airfoils (no camber), with different thicknesses. Figure 4 plots the c_p distributions of the NACA 0004 and NACA 0010, at zero angle of attack. Remember that the last two digits of the 4-digit NACA airfoil standard represent the maximum thickness, as a percentage of the chord length.

Question: In the above figure, which c_p curve corresponds to the NACA 0004 and which corresponds to the NACA 0010? Can the answer be determined by considering streamline curvature arguments?

For a symmetric airfoil at zero angle of attack, the curvature of the upper and lower surfaces are in opposite directions. The radii of curvature point in opposite directions as well. Since the farfield

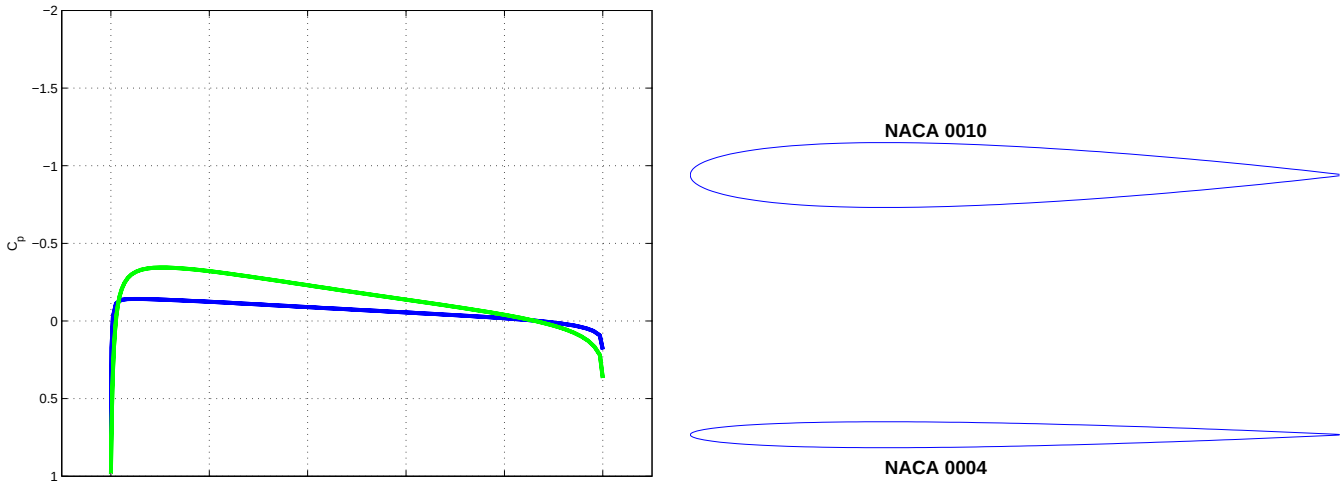

Figure 4: c_p distribution for NACA 0004 and NACA 0010 airfoils at zero angle of attack

pressure is p_∞ everywhere, and $\partial p/\partial n > 0$ for both surfaces. This means that pressure increases moving away from the airfoil (in the direction of the radius of curvature). This implies that the surface pressures, p_u on the upper surface and p_l on the lower surface, must be less than p_∞. The logic is,

$$\frac{\partial p}{\partial n} = \rho \frac{V^2}{R} > 0 \Rightarrow p_\infty - p_u > 0 \Rightarrow p_u < p_\infty.$$

Similarly, on the lower surface,

$$\frac{\partial p}{\partial n} = \rho \frac{V^2}{R} > 0 \Rightarrow p_\infty - p_l > 0 \Rightarrow p_l < p_\infty.$$

Thus, for a symmetric airfoil at zero angle of attack, the pressures on the surface are generally expected to be lower than p_∞, which is confirmed in the above plot. For a thicker airfoil, the radius of curvature is smaller, so the pressure gradient is larger, and the c_p reaches a more negative number (green line in Figure 4). Remember that the c_p plot is traditionally reversed on the y-axis. The

argument is that

$$\begin{aligned} R_{\text{thick}} &< R_{\text{thin}} \\ \frac{\partial p}{\partial n}_{\text{thick}} &> \frac{\partial p}{\partial n}_{\text{thin}} \\ p_{u_{\text{thick}}} &< p_{u_{\text{thin}}} \end{aligned}$$

Thickness therefore serves to generally increase the surface pressure gradient, while maintaining the same overall shape of the pressure distribution. We will examine the impact of thickness on cambered airfoils later.

2.2 The Leading-Edge Behavior

Consider the flow near the leading edge in the plot above. The leading edge is defined by the stagnation point of the flow, which corresponds to a $c_p = 1$.

Question: Why is the c_p value at a stagnation point equal to unity? Is this true for trailing edge stagnation points as well?

Since the leading edge is a stagnation point in the flow,

$$c_p \equiv \frac{p - p_\infty}{\frac{1}{2}\rho V_\infty^2} = \frac{\left(p_\infty + \frac{1}{2}\rho V_\infty^2\right) - p_\infty}{\frac{1}{2}\rho V_\infty^2} = 1$$

The trailing edge is also a stagnation point in the flow, but the plot above does not have $c_p = 1$ at the trailing edge. This is a purely numerical effect. The pressure distributions are computed using Xfoil, which is a panel method. As the panel resolution at the trailing edge increases, the c_p value would approach $c_p = 1$.

What happens when the flow around the symmetric airfoil is at a positive angle of attack? The c_p-distribution for the NACA 0004 at $\alpha = 3^\circ$ is shown in Figure 6a. At the leading edge, the pressure spikes and $c_p < -2$, which can be understood by considering the streamline curvature. For a positive angle of attack, the leading edge stagnation point is on the lower airfoil surface, as shown in Figure 5. The streamlines must therefore curve around the leading edge, which has a very small radius of curvature. As $R \to 0$,

$$\lim_{R \to 0} \frac{\partial p}{\partial n} = \rho \frac{V^2}{R} \to \infty.$$

Thus, the pressures at the leading edge will need to be very low to provide the required force to

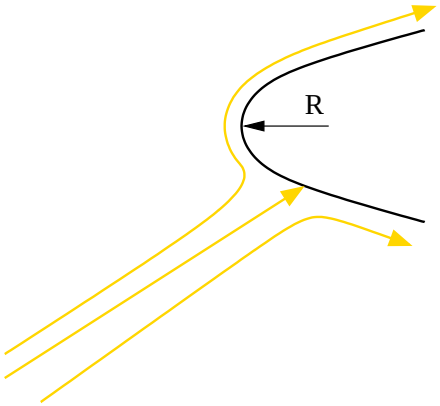

Figure 5: Streamlines near symmetric airfoil leading edge at a positive angle of attack.

turn the flow around the leading edge.

The leading edge pressure spike, as a result of flying the airfoil at a positive angle of attack, has also caused another effect: lift generation. The sharp decrease in pressure near the leading edge of the airfoil, explained by streamline curvature, leads to a net positive pressure integral in the y-direction. Thus, using streamline curvature and not Bernoulli, we have explained lift generation of an airfoil. We will make the same argument later as it relates to camber.

Question: What role does airfoil thickness play in the leading edge pressure spike?

Since the pressure spike is a manifestation of the small radius of curvature at the leading edge, a thicker airfoil will mitigate the spike. Consider the NACA 0010 at the same angle of attack in Figure 6b, where the strength of the pressure spike is clearly smaller.

For viscous flows, this strong pressure spike can lead to a separation of the upper surface boundary layer, which has implications for the stall performance of the airfoil. In addition to the leading edge thickness, another way to reduce this pressure spike is through the use of camber.

2.3 The Effect of Airfoil Camber

Adding camber is an effective method to reduce the leading edge pressure spike on an airfoil. The NACA 2404 has the same thickness as the NACA 0004, but has a 20% camber at $x = 0.4$. For the same lift coefficient, the cambered airfoil has virtually no pressure spike, as shown in the Figure 7a. However, too much camber can recover the pressure spike. Increasing the camber by another 20%

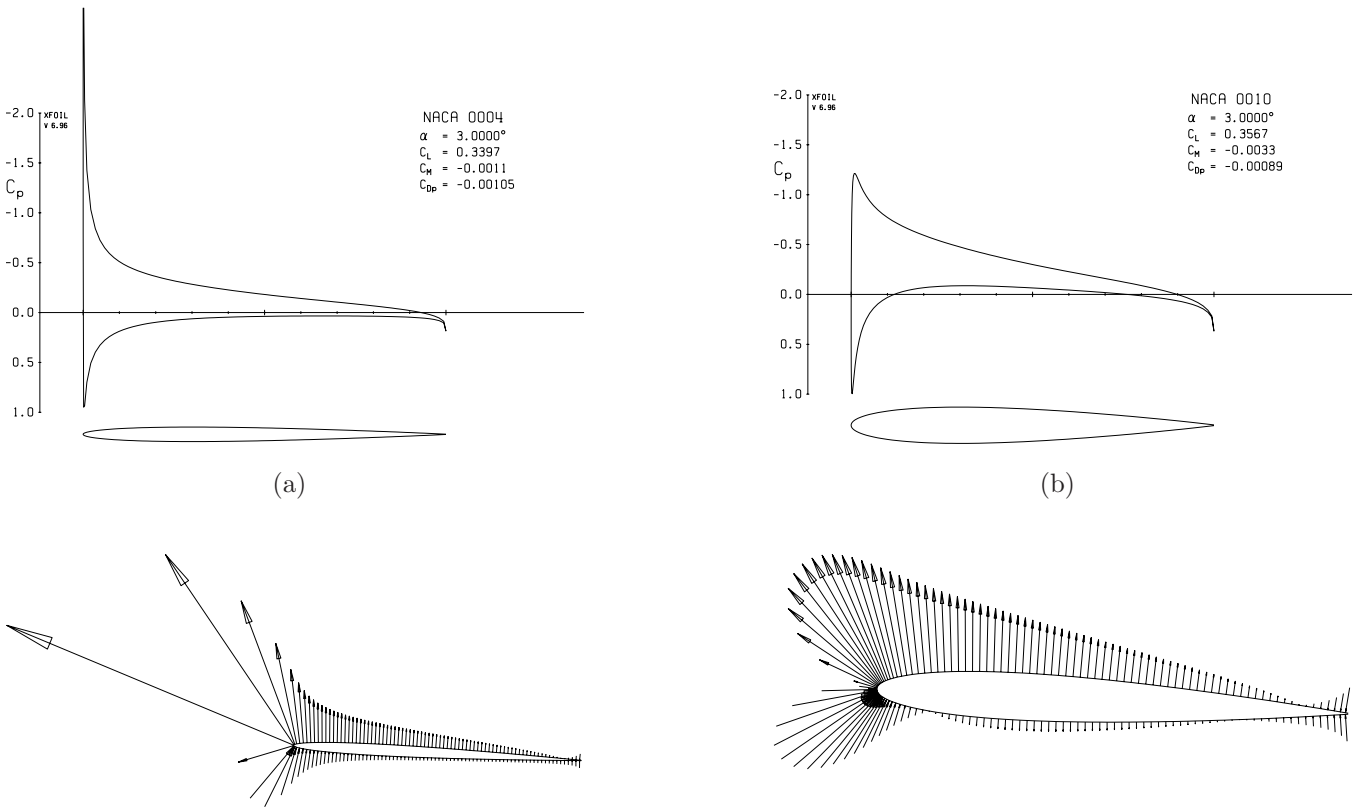

Figure 6: Pressure distribution for NACA 0004 and NACA 0010 at an angle of attack of $\alpha = 3°$.

to the NACA 4404 gives the c_p distribution shown in Figure 7b.

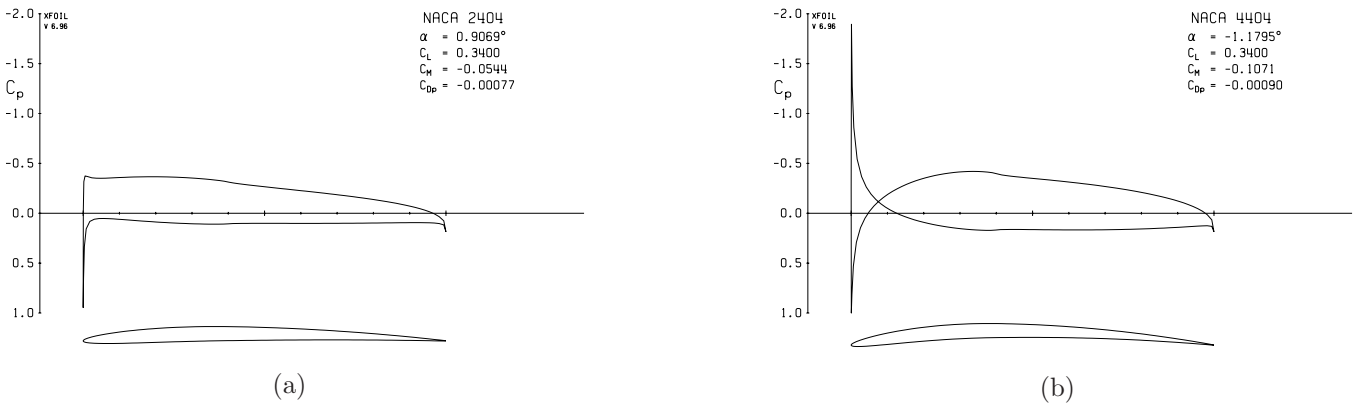

(a) (b)

Figure 7: The role of camber on the leading edge pressure spike for a NACA 2404 and NACA 4404 at the same c_l.

Question: Can you explain the difference in leading edge behavior between the NACA 2404 and NACA 5404 airfoils? Where is the leading edge stagnation point located on both airfoils?

The c_p distribution for the NACA 4404 shows the leading edge pressure spike on the *lower* surface curve. This is because the airfoil has too much camber for a small c_l, and the stagnation point is on the upper airfoil surface. Thus, the flow has to curve around a small radius of curvature to continue on the lower surface, leading to a pressure spike.

Beyond the leading edge behavior, The impact of camber on the pressure distribution of an airfoil can be qualitatively observed by considering an airfoil approximated by a single arc, such as seen below,

On the upper surface of the airfoil, which must be a streamline, $\partial p/\partial n > 0$, meaning that the pressure increases moving away from the airfoil. Since the farfield pressure is p_∞, this implies that $p_u < p_\infty$. The logic of the argument is,

$$\frac{\partial p}{\partial n} = \rho \frac{V^2}{R} > 0 \Rightarrow p_\infty - p_u > 0 \Rightarrow p_u < p_\infty.$$

Similarly, on the lower surface,

$$\frac{\partial p}{\partial n} = \rho \frac{V^2}{R} > 0 \Rightarrow p_l - p_\infty > 0 \Rightarrow p_l > p_\infty.$$

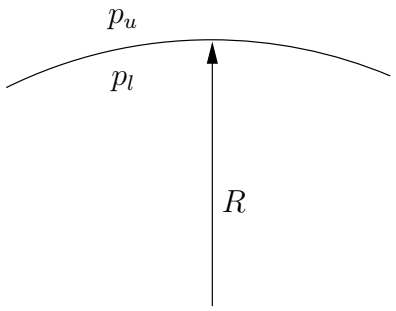

Figure 8: Airfoil with a circular arc camber line with radius R and zero thickness. p_u is the upper surface pressure, p_l is the lower surface pressure.

Combining these results which are solely based on the curvature of the surface, we see that $p_u < p_\infty < p_l$. Thus, this airfoil will generate lift since the pressure is lower on the upper surface than on the lower surface. This argument is why the upper airfoil surface is often referred to as the *suction* side of the airfoil and the lower airfoil surface is called the *pressure* side. Once again we have a net positive pressure integral in the y-direction and lift is generated.

As an example of the pressure distribution on a thin, circular arc airfoil, consider the NACA 4502 airfoil. The maximum camber is 4% of the chord and occurs at $x/c = 0.5$. Note: the NACA 4-digit series airfoils have camberlines which are two circular arcs that meet at the maximum camber location. Thus, when the maximum camber is at $x/c = 0.5$, the two circular arcs have the same radius. The c_p distribution for the 4502 at a $\alpha = 0$ is shown in Figure 9. The c_p distribution for the 4502 shows that the pressures are below p_∞ on the upper surface, and above p_∞ on the lower surface. Furthermore, the decrease in pressure on the upper surface is nearly equal to the increase in pressure on the lower surface which is reasonable since the radius of curvature is essentially the same on both the upper and lower surface.

Question: Now that you understand the role of both thickness and camber on streamline curvature of an airfoil, is the Thin Airfoil Theory assumption valid? Does the theory break down for airfoils with non-zero thickness?

Question: What role will increasing/decreasing the thickness play for a cambered airfoil? What will be the change in lift?

On a cambered airfoil, the trends with thickness are similar to the trends on a symmetric airfoil.

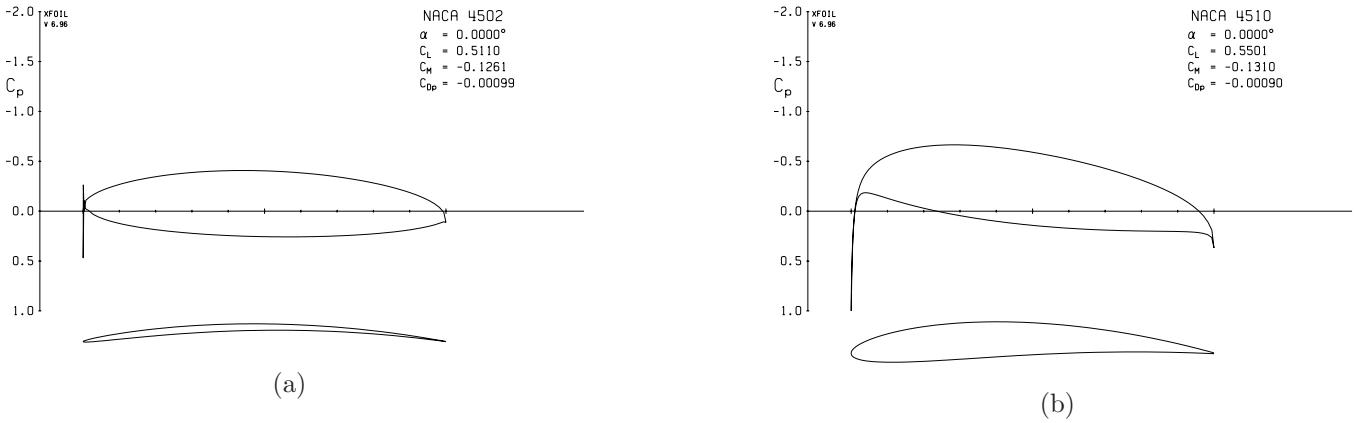

Figure 9: The impact of thickness on cambered airfoils for the NACA 4502 and NACA 4510 at $\alpha = 0°$.

Specifically, the addition of thickness will tend to lower the c_p on both sides of the airfoil. Once again, this qualitative behavior can be motivated using streamline curvature arguments. Increasing the thickness on a cambered airfoil will tend to decrease the radius of curvature of the upper surface, and increase the radius of curvature of the lower surface. Thus, we have the following logic chain, on the upper surface,

$$\tau \uparrow \quad R \downarrow \quad \frac{\partial p}{\partial n} = \rho \frac{V^2}{R} \uparrow \quad p_\infty - p_u \uparrow \quad p_u \downarrow .$$

Similarly, on the lower surface,

$$\tau \uparrow \quad R \uparrow \quad \frac{\partial p}{\partial n} = \rho \frac{V^2}{R} \downarrow \quad p_l - p_\infty \downarrow \quad p_l \downarrow .$$

Since the addition of thickness to a cambered airfoil tends to lower both the upper and lower surface pressure and the lift is an integral of the upper and lower surface pressure difference, the resulting lift will be relatively unaffected by thickness. These trends in c_p and c_l can be observed by comparing the 10% thick cambered NACA 4510 airfoil shown in Figure 9b to the 2% thick airfoil. Note: the thicker airfoils were simulated at the same angles of attack for the corresponding thinner airfoils. For these conditions, the 5 times increase in thickness from 2% to 10% changes the lift by less than 10%.